JOURNAL OF CATALYSIS 25, 212–222 (1972)

A Study of the Texture and Structure of Raney Nickel

P. FOUILLOUX, G. A. MARTIN, A. J. RENOUPREZ,
B. MORAWECK, B. IMELIK, AND M. PRETTRE

Institut de Recherches sur la Catalyse, 39 Bd du 11 Novembre 1918, 69-Villeurbanne, France

Received May 19, 1970

The texture of Raney nickel was simultaneously approached by nitrogen adsorption, magnetic measurements, X-ray diffraction line-broadening, X-ray small angle scattering and electron microscopy. The grain of Raney nickel, with a size larger than 1000 Å, takes the form of a collection of crystallites ranging in size from 25 to 150 Å, held together in the shape of a sponge. The average pore radius is 34 Å, but individual elements possessing an average radius of 7 to 8 Å also appear. Electron and X-ray diffraction patterns correspond to face-centered cubic nickel.

I. INTRODUCTION

Raney nickel has been the subject of considerable research since its discovery. In most cases, however, this research has sought to establish its suitability as a catalyst in a given process, or else the effort has been to produce as highly active a catalyst as possible by more or less empirical methods. The discrepancy in the published results is probably connected to the differences in composition of the catalysts, since it has been demonstrated (*1*)–(*3*) that these differences depend to a large extent on the alloy used. The latter in fact contains several phases, which do not necessarily show the same reactivity when attacked by an alkaline solution. Lastly, the conditions under which the same alloy is leached can produce variation of the percentage of aluminium and alumina in the catalyst. Only recently has attention been turned to the study of all the factors involved, from the preparation of the alloy, the structure of the catalyst (*1*, *2*, *4–6*), to its composition (*1*, *4*, *7*) and its texture (*6*).

As the conclusions on this subject clearly bring out (*5*, *7*), the differences in the composition of the various Raney nickels can explain the disparity in the published results concerning the quantities of hydrogen dissolved or adsorbed by this solid. Moreover, many hypotheses advanced to explain the presence of important quantities of hydrogen bonded to the catalyst have proved to be doubtful. For example, it seems that the presence of nickel hydride NiH_2 in important quantities can now no longer be postulated (*8*). These compounds have recently been synthesized and their lattice spacings are clearly different from that of nickel (*9*, *10*). For them to pass unseen on the X-ray diffraction pattern, they must be in an amorphous form.

Two types of technique have been used to determine the content of hydrogen in Raney nickel. The first is based on the chemical or electrochemical oxidation of the hydrogen in an aqueous medium. In this case there is a risk of oxidizing the nickel powder as well as the hydrogen (*11–13*):

$$Ni + 2\,H_2O \rightleftarrows Ni(OH)_2 + 2\,H_2$$
$$Ni + 2\,OH^- \rightleftarrows Ni(OH)_2 + 2\,e^-.$$

Generally, it can be postulated that any reactant SH is capable of producing a similar reaction:

$$Ni + 2\,SH \rightleftarrows Ni\,S_2 + H_2.$$

The residual aluminium may also react (*5*, *13*):

$$2\,Al + 6\,H_2O \rightleftarrows Al(OH)_3 + 3\,H_2,$$

in which case a systematic error is made by calculating to excess the quantity of hydrogen titrated.

The other type of technique is the thermal desorption of hydrogen. But unless special precautions are taken, the catalyst impregnating liquid may react with the aluminium and the nickel, which would explain certain violent and explosive reactions which accompany the heating of the solid (*5*, *14*). If care is taken to eliminate every trace of solvent, the quantity of hydrogen measured is always within the same range, for comparable catalysts.

For a complete study of the texture of Raney nickel, we used several physical techniques. First, nitrogen adsorption data at 77°K gave the specific surface and pore radius distribution. X-ray small angle experiments were made in order to measure pore and particle size especially in the range from 2 to 15 Å, while an X-ray line-broadening study was performed to discover whether particles shown by electron micrographs are polycrystallites. Then magnetic measurements pointed out the absence of very small particles. In the last part of the study, saturation magnetization values were related to the hydrogen adsorbed on nickel.

Each of the methods used makes it possible to bring out clearly only one aspect of the morphology of Raney nickel. But this aspect ought not to be viewed separately; only by confrontation of the different aspects can an idea of the entire problem be reached.

II. Preparation of Raney Nickel

The method followed for the preparation of the nickel (*1*) aims to eliminate as much aluminium as possible. The alloy is made up of very pure nickel and aluminium and titrates 46% of nickel. Finely ground, only the fraction of the particles with a diameter less than 40μ is kept for use. The catalyst is stabilized by storing for six months in a solution of normal soda.

III. Chemical Composition and Phase Identification by X-Rays and by Electron Diffraction

Raney nickel being pyrophoric, it is impossible to weigh it exposed to the air when it is dry. When it has been taken out of the normal soda, where it has been kept, it is washed in distilled water until neutrality. Then it is dried in vacuum for 12 hr in a bulb of Pyrex glass which has been weighed beforehand. The sample is heated to 300°C until a pressure of 10^{-4} Torr is obtained. Maintaining the vacuum, the part of the bulb containing the catalyst is closed.

The sealed part of the bulb is then broken open within a methanolic solution of bromine so that the nickel and aluminium can be titrated in their metallic state. Alumina and nickel oxide content are determined according to a method already described (*15*). The results are summed up in Table 1 where the proportions of different constituents are expressed in percentage of the total weight of the sample.

The total of components titrated is as much as 99.4 ± 0.5%. The results bring out that the elimination by leaching in solutions of soda of decreasing concentration is almost perfect. However, a certain quantity of aluminium metal remains, and cannot be eliminated by an attack by boiling 6 *N* soda. Furthermore nickel oxide is present in the sample. Its origin may be the decomposition of $Ni(OH)_2$ when the insoluble residue is heated on the Bunsen burner, in which case the nickel would

TABLE 1
Chemical Composition of Raney Nickel

Metals		Insoluble residue after bromination in methanol	
Ni	Al	Al_2O_3	NiO
95.4 ± 0.2	3.5 ± 0.1	0.03 ± 0.01	0.5 ± 0.1

have begun to oxidize in water, according to the equation quoted above. In any case, this would only represent 1.67 cm^3 of hydrogen per gram of catalyst.

Phase identification was achieved by the Debye-Scherrer technique, using a 114 mm camera. A Lindemann glass capillary tube is filled with water to make the nickel particles slide more easily. The capillary is filled right up by packing in the damp powder with spun glass. After water has been drained off, the capillary is sealed without returning to the air. The diffraction lines have been indexed in Table 2 and are of face-centered cubic nickel.

A special method also had to be used in the preparation of the samples examined by electron diffraction, by reason of the pyrophoric nature of Raney nickel. After being washed in acetone, the catalyst was immersed in a solution of collodion. The film formed by the disappearance of the solvent was skimmed off onto a copper grid and kept wet until it was put into the microscope. By preparing the samples in this way, the nickel particles can be covered and kept away from the air. The diffraction patterns correspond to face-centered cubic nickel. Some of them reveal that all their crystallites are pointed in one direction. This can be explained on the assumption that the (110) plane is perpendicular to the electron beam (*16*). Two supplementary spots that can be seen were interpreted as arising from a rotation of certain elements. All the patterns do not show this preferential orientation since in a certain number of cases we observed simple powder patterns.

TABLE 2

SPACINGS OF THE CRYSTAL PLANES, SURFACE AVERAGE DIAMETER AND AVERAGE VOLUME OF THE CRYSTALLITES

Plane	Spacings of the crystal planes (Å)	Intensity of the lines	$\overline{D}_s$ (Å)	$\overline{D}_v$ (Å)
(111)	2.084	100	38.6	71.8
(200)	1.762	42	31.7	52.7
(220)	1.243	21	31.5	52.6

IV. STUDY OF THE TEXTURE OF RANEY NICKEL BY NITROGEN ADSORPTION–DESORPTION ISOTHERMS

Adsorption of nitrogen at 77°K was measured gravimetrically with a McBain balance with electronic compensation. The body of the balance can be connected either to a high vacuum line or to a tank of very pure nitrogen.

The sample is first dried at room temperature in the balance, until a pressure of 10^{-4} Torr is attained: the graph recording the loss of weight at this point straightens out. A large part of water is thus eliminated, otherwise it might react with the catalyst during the subsequent thermal treatment. The temperature is raised to 100°C for one of the experiments, and to 195°C for the other until loss of weight ceases. Applying the Brunauer, Emmett, and Teller equation (*17*) to the subsequent N_2 isotherms surface areas of 67 m^2/g or 78 m^2/g were obtained, depending on whether the final degassing temperature was 100°C or 195°C.

The N_2 adsorption isotherms are of type IV in the Brunauer classification (*18*), as had already been shown (*6*): they present a hysteresis which indicates the existence of an open porosity (Figs. 1 and 2). Tables (*10*), calculated according to Pierce's method (*20*), using Halsey's equation for the thickness of the multilayer (*21*), facilitate the calculation of the radii distribution of the pores in Raney nickel starting from the desorption branch of the isotherm. If V_p is the volume of pores of average radius $\bar{r}_p$, the graphs of Fig. 3, representing the fraction $\Delta V_p/\Delta \bar{r}_p f = (r_p)$ give the frequency of the pore radii. It can be seen that pores having a radius of 32 Å are the most abundant for the catalyst pretreated *in vacuo* at 100°C. For treatment at 195°C, the most numerous pores are those which have a radius of 26 Å (Fig. 3).

The cumulative surface area of the pores calculated up to the end point of hysteresis corresponds to the specific surface area with a margin of about 2 m^2/g for the catalyst pretreated *in vacuo* at 100°C.

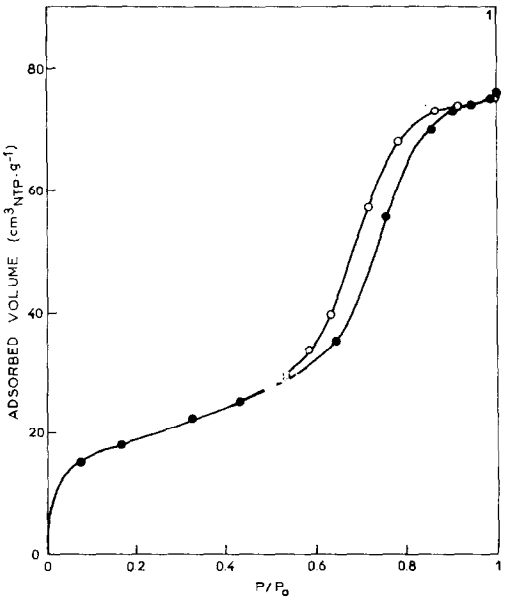

FIG. 1. Nitrogen adsorption–desorption isotherm on Raney nickel pretreated *in vacuo* at 100°C.

This implies that micropores (< 20 Å) are not present in the sample. The cumulative surface area calculated for the sample preheated *in vacuo* at 195°C is 10% greater than the specific surface determined by the BET method. This difference is somewhat higher than the error generally found for this type of isotherm. If this difference has any meaning it would indicate the presence of a slight amount of interconnected bottle-shaped pores (*22*), or a certain reversible mobility of the particles building blocks, in Raney nickel (*23*). The increase of surface area observed when pretreating the sample at 195°C may be due to the elimination of last traces of water.

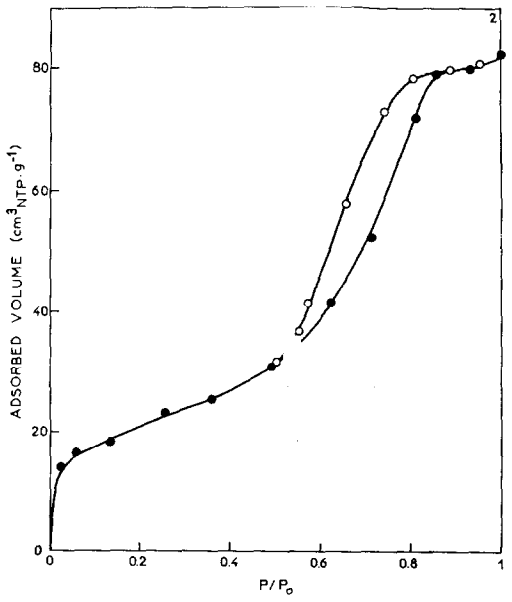

FIG. 2. Nitrogen adsorption–desorption isotherm on Raney nickel pretreated *in vacuo* at 195°C.

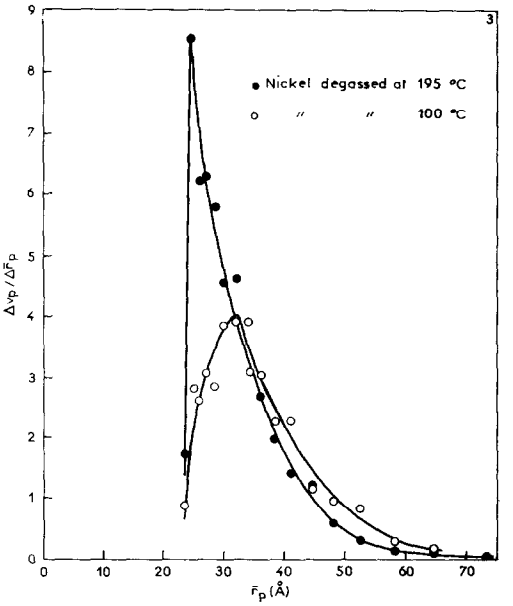

FIG. 3. Pore size distribution for Raney nickel.

In conclusion, gas adsorption experiments show us that the texture of Raney nickel is rather well defined with a narrow pore size distribution. Other methods have been used in order to sustain this hypothesis.

V. Magnetic Study of Raney Nickel Texture

The specific magnetization σ of Raney nickel has been measured in fields of up to 20,000 Oe. at various temperatures by the "axial extraction method" (*24*). In order to avoid the movement of particles in the magnetic field, the wet samples are tightly compressed.

The remanent and the saturation mag-

TABLE 3
REMANENT AND SATURATION MAGNETIZATION OF RANEY NICKEL IN DIFFERENT AQUEOUS MEDIA

Aqueous medium	σ_s gauss cm³/g catalyst	σ_r gauss cm³/g catalyst
Distilled water	28.9	3.75
Buffer pH 7.0	29.5	4.0
Normal soda	30.3	4.0

netization, σ_r and σ_s, of the catalyst in different aqueous media do not vary in any significant way. Table 3, where the magnetic moments per unit mass at 298°K are listed, indicates that the interaction between the metal and the water seems to be small. It is possible to observe the sintering of Raney nickel during a thermal treatment; the relationship between σ/σ_s and the magnetic field H at high field is (*25*):

$$\sigma/\sigma_s = 1 - (kT/\mu H)$$

N being the number of nickel atoms in the metal particle, and β the Bohr magneton, $\mu = 0.606\ N\beta$. For nickel N will be related to the diameter (in Å) of the particles thought to be spherical by:

$$N = 0.0477\ d^3$$

The slopes of the lines in Fig. 4 relate to

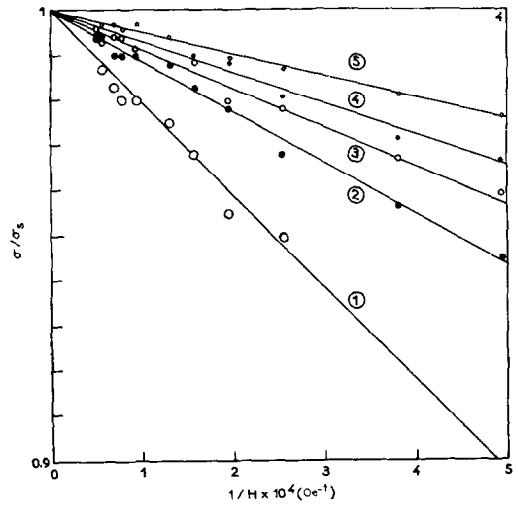

FIG. 4. Degree of saturation magnetization for Raney nickel as a function of magnetic field.

Raney nickel before treatment, then heated at 112, 176, 350 and 600°C (respectively, curves 1, 2, 3, 4, 5). The mean diameters calculated from the slopes are 93, 112, 125, 140 and 150 Å and give a rough idea of the sintering. The coercive field and the saturation magnetization of the Raney nickel before desorption of hydrogen, were measured at various temperatures (Table 4). The coercive field approaches 300 Oe at low temperature, a figure which has been observed for nickel powder. It should be noticed that fields of 1500 Oe are observed whenever the particles are rodlike in shape and the ratio of their length to their diameter is equal to ten (*26*), which indicates in the present case that the small particles have almost a regular shape. It was also observed that the saturation magnetization increased in the same proportion as for bulk nickel, when the temperature decreases from 77 to 1.6°K (34 and 34.6 for Raney nickel, 56.8 and 57.4 for bulk nickel). It can be concluded that the percentage of very finely divided particles smaller than 15 Å in diameter, which are unsaturated at 77°K, is negligible.

VI. STUDY OF THE TEXTURE BY X-RAYS

Two kinds of experiments were performed on Raney nickel, viz., line-broadening analysis in order to determine the crystallite size, and small-angle scattering for the pore and particle size measurements.

Diffraction profiles were measured by step scanning using a diffractometer equipped with a scintillation counter and a monochromator isolating the $K\alpha_1$ radiation of copper. The sample (diameter $\sim$ 2 cm)

TABLE 4
COERCIVE FIELD AND SATURATION OF THE RANEY NICKEL AT VARIOUS TEMPERATURES

T(°K)	H_0(Oe)	σ_s (gauss cm³/g)
298	32	29
77	146	34
4.2	300	34.6
2.2	300	34.6
1.6	—	34.6

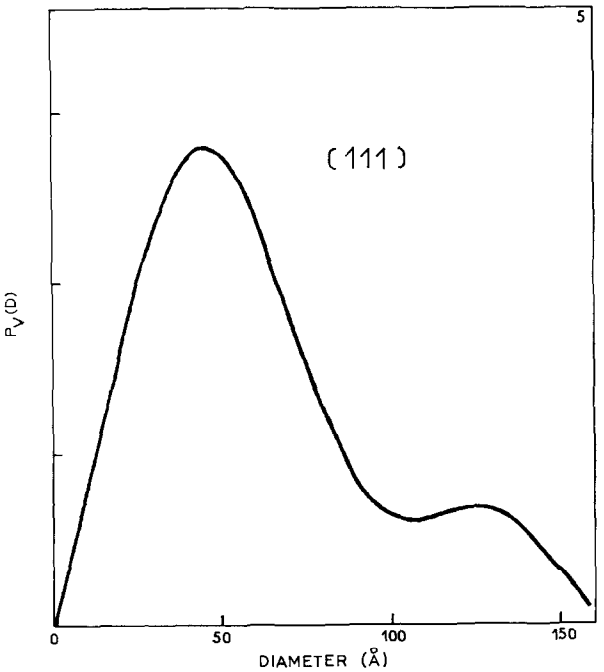

FIG. 5. Volume distribution of crystallites as a function of their diameter perpendicular to the plane (111), from X-ray line-broadening.

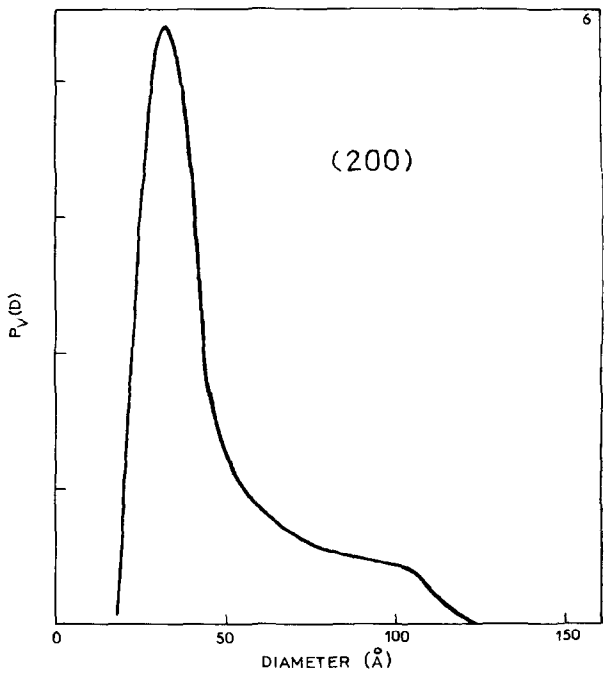

FIG. 6. Volume distribution of crystallites as a function of their diameter perpendicular to the plane (200), from X-ray line-broadening.

was protected from oxidation by coating it immediately with a thin film of collodion; a check was made before and after the experiment that no diffraction line of NiO or $Ni(OH)_2$ appeared.

The experimental profiles were corrected by Fourier analysis thanks to the Stokes method (*27*) using as a reference sample a Mond nickel powder. The slope at the origin of the Fourier transform for the corrected profile gives a surface average diameter $\overline{D_s}$ (*27*) of the crystallites lying perpendicular to the plane in question (*28*). The integral breadth of the corrected profile gives an average volume $\overline{D_v}$ for these diameters. Table 2 summarizes the results obtained for the (111), (200) and (220) lines. Quite a marked anisotropy is noticeable since for the (111) plane $\overline{D_v}$ is 40% higher than for the (200) or (220) plane.

By calculating the second derivative of the Fourier transform for the corrected profile, we can determine the complete distribution of crystallite diameters. These distributions are plotted in Figs. 5 and 6 for the (111) and (200) planes: they show that diameters vary between 25 and 150 Å.

Small angle X-ray experiments were performed with a low angle goniometer (*29*); the Cu $K\alpha_1$ radiation is focused on the detector slit with a 1400 mm curvature quartz monochromator. As Raney nickel is pyrophoric, it has to be kept soaked in water inside the sample holder.

The intensity distribution curve obtained step by step with the goniometer enables us to calculate the surface area and the distribution of the radii of the heterogeneities in the solid (*30*). Figures 7 and 8 show the distribution of the diameter as a function of the surface or of the volume to which they contribute (solid line). They present a first maximum at 70 Å, which is in good agreement with pore size observed from the adsorption isotherm after desorption of Raney nickel at 100°C. But another maximum appears at 7–8 Å. The surface area included between the diameter axis and the curve in Fig. 7 is proportional to

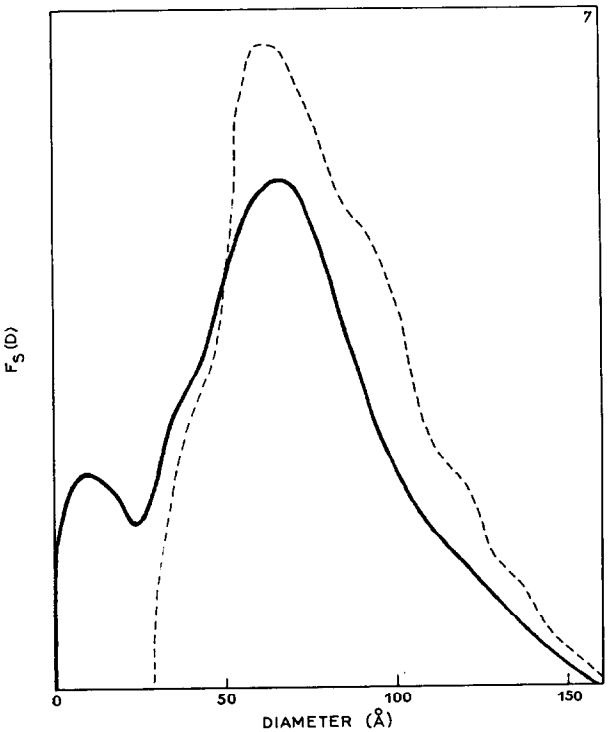

FIG. 7. Heterogeneities (surface distribution) from small angle X-ray scattering for Raney nickel powder not compressed (full line) and compressed under 1 Ton/cm² (dotted line).

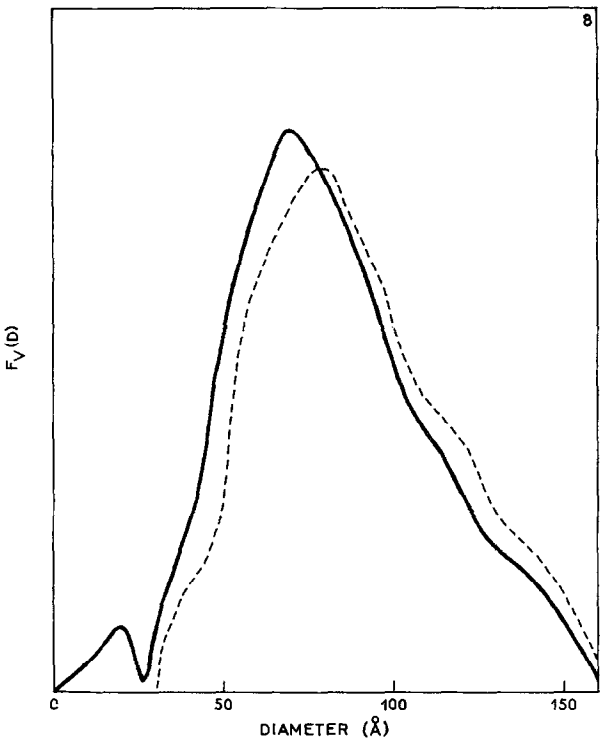

FIG. 8. Heterogeneities (volume distribution) from small-angle X-ray scattering for the Raney nickel powder not compressed (full line) and compressed under 1 Ton/cm² (dotted line).

the surface area of the catalyst. The surface measured by nitrogen was due to the pores with a radius greater than 20 Å; the small-angle scattering shows that a certain part of the surface is made up of pores with a radius less than 20 Å. We calculate the ratio of the total specific surface developed by these micropores to be 25%. Another experiment was performed on a compressed sample (1 Ton/cm²). The curves in Figs. 7 and 8 (dotted line) show that there is no maximum in the range 0–20 Å. This fact corroborates the assumption of the mobility of the texture. The smallest heterogeneities are probably fractures between crystallites which disappear when the sample is compressed as indicated above.

VII. Study of the Catalyst by Electron Microscopy

Electron diffraction and electron microscopy were operated simultaneously for each grain examined.

Raney nickel has the form of porous sponge bored with little holes whose diameter, about 70 Å, corresponds to the diameter of the pores measured by the preceding methods and to the description of a nickel of the same type which appeared in a recent publication (*16*). The large particles have diameters ranging up to several microns. Some authors (*31*, *32*) have noticed grains of a different appearance. However the presence of NiO on their diffraction pattern shows that the Raney nickel had been oxidized, which perhaps modified its texture.

VIII. Volume of Hydrogen Adsorbed and Content of Aluminium Related to Saturation Magnetization

The desorption of the hydrogen has a marked influence on magnetic properties. Nickel, washed with distilled water, is compressed into a transparent quartz tube. At the beginning of the experiment the sample is dried *in vacuo* at 23°C. A part of the hydrogen is desorbed under vacuum at the same temperature and the water is trapped by liquid nitrogen. The desorbed

hydrogen is forced back into the rough vacuum tank which has previously been isolated from the rotary pump. The pressure increments measured on a McLeod gauge are proportional to the quantities of hydrogen desorbed. Mass spectrometry made it possible to check that this increase in pressure was due to hydrogen, to exclusion of any other gas. Figure 9 shows the quantities of hydrogen desorbed down to a pressure of 10^{-6} Torr, and for higher and higher temperature levels. At the same time, the magnetic moment per unit mass, σ_s, is measured at 298 and 4.2°K. In Fig. 10, σ_s is shown as a function of the volume v of hydrogen desorbed per gram of catalyst. The graphs are two straight lines over an important section of their length, which indicates no change in the nature of the bond between H_2 and Ni. If some hydrogen is readsorbed, the magnetization is decreased and the slope is still the same.

It can be said that:

$$d\sigma_s/dv = \mathfrak{N}\alpha\beta/22\,414$$

$\mathfrak{N}$ is the Avogadro number and α is the variation of specific magnetization in Bohr magnetons (β) per molecule of hydrogen adsorbed. If a surface hydride NiH is formed, α will be equal to $2 \times 0.6 = 1.2$. When σ_s is measured at 298°K, the calculated α value is 1.18 (or 1.23 if the temperature variations for σ_s are taken into account). At 4.2°K, α is 1.10. At 298°K, very small particles may be unsaturated so that an important error is possible in determining α. At 4.2°K, all nickel is saturated, but the nature of the binding may be changed by such a cooling. Yet for the two cases we have attained a large agreement with the theoretical results and we can conclude that the hydrogen–nickel bond is of the type NiH, a hypothesis already advanced with regard to Raney nickel (*4*) and supported nickel catalysts.

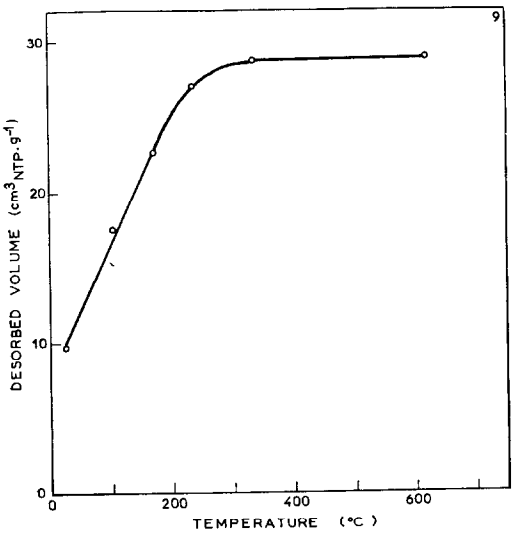

FIG. 9. Volume of hydrogen desorbed *in vacuo* as a function of temperature.

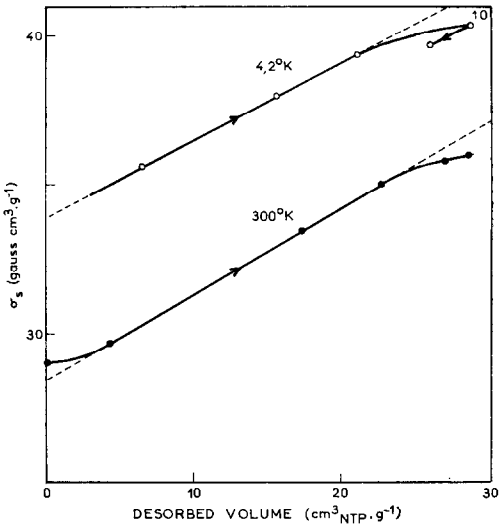

FIG. 10. Variation of saturation magnetization as a function of the volume of hydrogen desorbed.

The adsorption of H_2 on the Raney nickel is dissociative and there may occur either equal distribution of the number of nickel atoms belonging to the planes (100), (110), (111) or equal distribution of the surfaces of these planes. In the first alternative, 1 cm³ of hydrogen will saturate a surface of 3.64 m², in the second a surface of 3.30 m² of the catalyst. Since the volume of hydrogen desorbed per gram of catalyst is 29.5 cm³, according to whether we take the first or the second hypothesis, the surface will be in the range from 98 to 107 m²/g, if all the hydrogen is adsorbed on the surface. These values are in relatively good agreement with the BET surface. Figure 10 reveals that when all the hydro-

gen is desorbed, the magnetic moment per unit mass is only 40.4 gauss cm^3/g at 4.2°K instead of 57.4 for massive and pure nickel. Raney nickel contains 3.5% metallic aluminum. Supposing that each atom of aluminum diminishes the saturation magnetization of nickel by exchange of electrons, α' representing the variation of magnetic moment in Bohr magnetons per atom of aluminum, the variation $\Delta\sigma_s$ of saturation magnetization for one gram of the sample will be:

$$\Delta\sigma_s = \mathfrak{N}\alpha'(m/M)$$

m: mass of aluminum per gram of nickel
M: atomic mass of aluminum

$$\Delta\sigma_s = 57.4 - 40.4 = 17.0 \text{ gauss } cm^3/g$$

The calculations give $\alpha' = 2.4 \pm 0.2$ Bohr magnetons. Now it has been proved (*33–35*) that if a nonferromagnetic metal is dissolved in nickel in the state of impurity, α' is equal to the valency of the metal dissolved. For aluminum α' should be equal to 3. We conclude that aluminum metal is present in Raney nickel in the form of solid solution.

IX. Conclusion

The specific surface area obtained by BET method after desorption at 100°C *in vacuo* is 67 m^2/g; after desorption at 195°C a value of 78 m^2/g is observed. This increase may be due either to the fact that the small crystallites which make up the large aggregates have fallen apart, or to the elimination of last traces of water.

The volume of hydrogen collected by thermodesorption *in vacuo* would give a minimal specific surface of 98 to 107 m^2/g on the assumption that this hydrogen is adsorbed in the form of a surface hydride NiH, as shown by magnetic measurements.

The distribution of the sizes of the heterogeneities in the solid emerging from the data of X-ray small-angle scattering shows that damp nickel has an average pore radius of 34 Å, which is in perfect agreement with that calculated from the nitrogen desorption branch at the temperature of liquid nitrogen. But individual elements possessing an average radius of 7–8 Å also appear. Saturation magnetization at low temperature suggests that they are microfractures between crystallites rather than very small particles.

From the point of view of texture, the grain of Raney nickel with a size larger than 1000 Å takes the form of a collection of crystallites ranging in size from 25 to 150 Å, adhering together in the shape of a sponge. The interior surface of this sponge, which is esentially a pore surface, measures 78 m^2/g.

Chemical analysis having shown that there is about 3% aluminum metal in our Raney nickel, it is probable that the solid solution formed is imperfect and that there exist accumulations of several aluminum atoms favoring the formation of micropores full of hydrogen. These pores at the heart of the metallic lattice have great difficulty communicating with the surface.

On the other hand, the nitrogen adsorption isotherm does not reveal any pores less than 20 Å in radius. But if the figure 78 m^2/g obtained by the BET method is multiplied by the coefficient 1.28 obtained by small-angle scattering, making it possible to take into account the surface corresponding to micropores, a result of 100 m^2/g is obtained. This surface in fact lies within 98 and 107 m^2/g (calculated by mean of the volume of hydrogen desorbed).

The preceding hypotheses explain the results taken as a whole, but the reservations that can be made in their regard must not be forgotten. In particular all the hydrogen was considered as being fixed on the surface, when in fact a part might have been dissolved in the deeper layers when preparing the solid (*11*). Even so, it must be said than below 140 atm. and at 400°C, the quantity absorbed by a nickel of the Raney type according to this process is only 0.4 cm^3/g (*4*). Likewise a small volume of hydrogen adsorbed in the form of NiH_2, would change the results of the calculations in quite a similar way. Neither is it certain that the planes (100), (110), (111), are equally exposed on the surface of the solid.

In spite of the limitations pointed out, the results as a whole, gathered from

samples taken from the same batch of catalyst, do shed light on the intimate make-up of Raney nickel.

REFERENCES

1. SASSOULAS, R., AND TRAMBOUZE, Y., *Bull. Soc. Chim.* **5**, 985 (1964).
2. KAGAN, A. S., KAGAN, H. M., TCHIJIK, S. P., OULIANOVA, G. D., AND CHICHKINE, A. B., *Dokl. Akad. Nauk. SSSR* **185**, 1104 (1969).
3. FREEL, J., PIETERS, W. J. M., AND ANDERSON, R. B., *J. Catal.* **14**, 247 (1969); **16**, 281 (1970).
4. KOKES, R. J., AND EMMETT, P. H., *J. Amer. Chem. Soc.* **81**, 5032 (1959).
5. MARS, P., SCHOLTEN, J. J. F., AND ZWIETERING, P., "Actes 2ème Congrès Internationale Catalyse" p. 1245. Editions Technip, Paris, 1960.
6. BEZAUDUN, J., Thèse, Lyon, 1964.
7. JAMEY, J. P., Thèse, Lyon, 1966.
8. RANEY, M., *Ind. Eng. Chem.* **32**, 1199 (1940).
9. MASCHRZAK, S., *Bull. Acad. Pol. Sci. Ser. Sci. Chim.* **10**, 485 (1967).
10. JANKO, A., AND PIELASZEK, J., *Bull. Acad. Pol. Sci. Ser. Sci. Chim.* **11**, 569 (1967).
11. PRETTRE, M., *C. R. Acad. Sci.* **265C**, 957 (1967).
12. BEZAUDUN, J., DALMAI, G., AND PRETTRE, M., *C. R. Acad. Sci.* **258**, 1779 (1964).
13. HORANYI, G., AND NAGY, F., *Mag. Chem. Folyoirat* **70**, 475 (1964).
14. SMITH, H. A., CHADWELL, A. J., AND KIRSLIS, S. S., *J. Phys. Chem.* **59**, 820 (1955).
15. JAMEY, J. P., URBAIN, H., AND TRAMBOUZE, Y., *Bull. Soc. Chim.* **9**, 2777 (1966).
16. KNAPPWOST, A., AND MADER, K. H., *Naturwissenschaften* **52**, 590 (1965).
17. BRUNAUER, S., EMMETT, P. H., AND TELLER, E. J., *J. Amer. Chem. Soc.* **60**, 309 (1938).
18. BRUNAUER, S., "The Adsorption of Gases and Vapors." Oxford University Press, London, 1953.
19. IMELIK, B., AND FRANCOIS-ROSSETTI, J., *Bull. Soc. Chim.* **24**, 153 (1957).
20. PIERCE, C., *J. Phys. Chem.* **57**, 149 (1953).
21. HALSEY, G. D., *J. Chem. Phys.* **16**, 931 (1948).
22. DE BOER, J. H., VAN DER HENVEL, A., AND LINSEN, B. G., *J. Catal.* **3**, 268 (1964); RENOU, J., Thèse, Paris, 1960.
23. BARRER, R. M., AND MCLEOD, D. M., *Trans. Faraday Soc.* **51**, 1290 (1955).
24. PAUTHENET, R., *Ann. Phys.* **7**, 710 (1952).
25. MARTIN, G. A., *J. Chim. Phys.* **66**, 140 (1969).
26. NEEL, L., *J. Phys. Rad.* **5**, 241 (1944).
27. GUINIER, A., "Théorie et Pratique de la Radiocristallographie," p. 462. Dunod, Paris, 1964.
28. MORAWECK, B., AND RENOUPREZ, A. J., *C. R. Acad. Sci.* **266B**, 1075 (1968).
29. RENOUPREZ, A., WEIGEL, D., AND IMELIK, B., *J. Chim. Phys.* **62**, 131 (1965).
30. DONATI, J., PASCAL, B., AND RENOUPREZ, A. J., *Bull. Soc. Fr. Cristallogr.* **XC**, 452 (1967).
31. YASUMURA, J., *Nature* **173**, 80 (1954).
32. YAMAGUSHI, S., *Z. Phys. Chem.* **211**, 358 (1959).
33. HEDLE, T. A., *Brit. J. Appl. Phys.* **4**, 161 (1964).
34. STONER, E. C., *Phil. Mag.* **15**, 1018 (1933).
35. BOZORTH, R. M., "Ferromagnetism," p. 440. D. Van Nostrand, New York, 1964.